IEEE Photonics Journal
An IEEE Photonics Society Publication

Open Access

Broadband Microwave Spectrum Sensing Based on Photonic RF Channelization and Compressive Sampling

Volume 12, Number 1, February 2020

Bo Yang
Hao Chi, *Senior Member, IEEE*
Shuna Yang
Zizheng Cao
Jun Ou
Yanrong Zhai

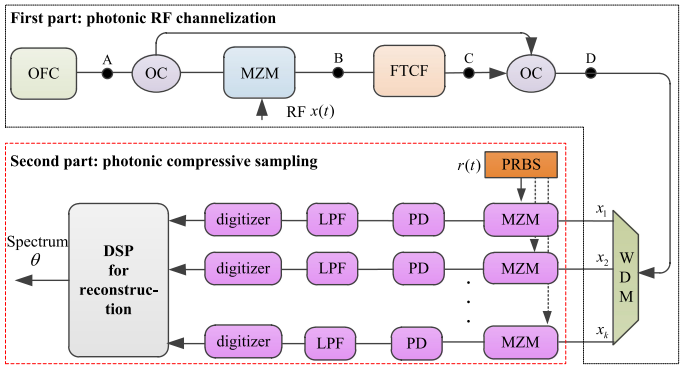

DOI: 10.1109/JPHOT.2019.2960377

Broadband Microwave Spectrum Sensing Based on Photonic RF Channelization and Compressive Sampling

Bo Yang,[1] **Hao Chi**,[1] ***Senior Member, IEEE***, **Shuna Yang**,[1] **Zizheng Cao**,[2] **Jun Ou**,[1] **and Yanrong Zhai**[1]

[1]School of Communication Engineering, Hangzhou Dianzi University, Hangzhou 310018, China
[2]COBRA Institute, Eindhoven University of Technology, Eindhoven 5600 MB, The Netherlands

DOI:10.1109/JPHOT.2019.2960377

Manuscript received November 24, 2019; revised December 5, 2019; accepted December 14, 2019. Date of publication December 19, 2019; date of current version January 7, 2020. This work was supported in part by the National Key R&D Program of China under Grant 2019YFB2203204, in part by the National Natural Science Foundation of China under Grants 61975048, 61901148, and 41905024, and in part by the Zhejiang Provincial Natural Science Foundation of China under Grants LQ20F010008, LZ20F010003 and LQ18F050002. Corresponding author: Hao Chi (e-mail: chihao@hdu.edu.cn).

Abstract: A novel approach to realize broadband microwave spectrum sensing based on photonic RF channelization and compressive sampling (CS) is proposed. The photonic RF channelization system is used to slice the input broadband signal into multiple sub-channel signals with narrow bandwidth in parallel and thus the rate of pseudo-random binary sequence (PRBS) and the bandwidth of the MZM for CS can be largely decreased. It is shown that a spectrally sparse signal within a wide bandwidth can be captured with a sampling rate far lower than the Nyquist rate thanks to both photonic RF channelization and CS. In addition, the influence of the non-ideal filtering of the photonic channelizer is evaluated and a novel approach based on measuring twice is proposed to overcome the problem of frequency aliasing induced by the non-ideal filtering. It is demonstrated that a system with 20 Gbit/s PRBS and 2.5 GS/s digitizer can be used to capture a signal with multiple tones within a 40 GHz bandwidth, which means a sampling rate 32 times lower than the Nyquist rate.

Index Terms: Photonic RF channelization, compressive sampling, microwave photonics.

1. Introduction

Microwave signal processing with photonic technology has attracted much interest owing to the advantages of wide bandwidth, low loss, and immunity to electromagnetic interference offered by photonics. In modern wireless communications and advanced radar system, it is necessary to analyze the spectrum of the received microwave signals within a large bandwidth. Photonics-based approaches for microwave spectrum analysis are considered as competitive alternatives since conventional electronic techniques are limited by the inherent bandwidth bottleneck. In recent years, a variety of photonics-based approaches for microwave spectrum sensing have been proposed [1]–[28]. These approaches can be roughly divided into four categories: photonic instantaneous frequency measurement [1]–[4], spectrum analysis based on optical frequency scanning [5]–[7], photonic RF channelization [8]–[15], and photonic-assisted analog-to-digital conversion (ADC) [16]–[28]. Photonic RF channelization can slice the input broadband signal into sub-channels with

narrow bandwidth and support spectrum measurement of microwave signal with a large bandwidth, however its resolution is usually limited by the minimum achievable bandwidth of the optical filter (typically larger than 1 GHz). Especially, photonic-assisted ADC is of great interest because it can not only support a wide bandwidth measurement but also features high-resolution and high-sensitivity. Recently, photonic-assisted ADC based on compressive sampling (CS) provides a potential solution for broadband microwave spectrum sensing with sub-Nyquist sampling rate [21]–[29]. According to the theory of CS, it is possible to recover a signal with sampling points far less than that demanded by the Nyquist theorem given that the signal is sparse in a certain orthogonal basis [30]. A spectrally sparse signal composed of a few sinusoidal signals can be captured in a periodical sampling mode with CS based schemes, such as the modulated wideband converter (MWC) and the random demodulator [30], [31]. The photonic CS based on random demodulator aims to capture sparse multitone signals with simple structure [21] while the MWC-based photonic CS is preferred for the capture of sparse multiband signals with good approximation [22]. These two schemes both involve random mixing, low-pass filtering, and down-sampling, while differ in the structure, recovery algorithm, and assumed signal model. In the random mixing stage, the signal of interest must be multiplied with a pseudo-random binary sequence (PRBS) at or above its Nyquist rate, which may be a challenge in the applications with ultrahigh bandwidth. Several schemes have been proposed to overcome this challenge based on the approaches of optical mixing [26], photonic time stretch/compression [27], [28]. In [26], an optical mixing scheme for realizing the MWC or the random demodulator is proposed to avoid high speed electronics, the PRBS is recorded in the frequency domain by using a spectrum shaper with spatial light modulator (SLM). Since the length of the PRBS affects the signal recovery performance in CS, the upper limit of the length of PRBS that can be recorded in an SLM is further investigated in [29]. In [27], an approach to realizing microwave spectrum sensing based on photonic time stretch and CS is proposed, the signal to be measured is slowed down in the time domain by photonic time stretch and therefore the rate of the applied PRBS can be decreased. In [28], the technique of photonic time compression is applied to accelerate the PRBS and increase the effective sampling rate in CS, where the PRBS modulated highly chirped ultrafast laser pulses is partially compressed in time before sampling the microwave signal. However, the continuous-time operation in photonic time stretch/compression is complex and hard to realize.

In this Letter, we propose a novel spectrum sensing scheme for broadband microwave signal that combines the advantages of photonic RF channelization and CS. The input broadband signal is firstly sliced into a bank of sub-channels by a photonic RF channelizer and then the microwave signal in each sub-channel is processed and captured by a random demodulator based photonic CS module. In the scheme, all the photonic CS modules share a same PRBS generator and the clock rate of the PRBS as well as the speed of mixer is largely decreased, which is highly desired in practical realizations of CS. A sampling rate much lower than the Nyquist rate, as a result of the photonic RF channelizer and the CS, is sufficient for reconstruction of broadband microwave signals with high frequency resolution. In addition, we also propose a novel approach based on measuring twice with different ranges of alias frequency to eliminate the problem of spectral leakage induced by the non-ideal filtering in the photonic channelizer. It is shown that a system with a 20 Gbit/s PRBS and a 2.5 GS/s digitizer can be used to capture a signal with multiple tones in a 40 GHz bandwidth.

2. Operation Principle

The proposed scheme is schematically illustrated in Fig. 1. The system is composed of two parts. The first part is a photonic RF channelization system, which acts like a vernier caliper based on an optical frequency comb (OFC) and a flat top optical comb filter (FTCF) with different spacings. The operation principle of the photonic RF channelization is similar to the proposals in [12], [13], except that the OFC is reused as optical reference for heterodyne detection in this scheme and the exact spectral information can be obtained by the followed CS. As shown in Fig. 1(a), an OFC is chosen as the light source of the photonic channelizer and split into two paths by an optical coupler (OC). In

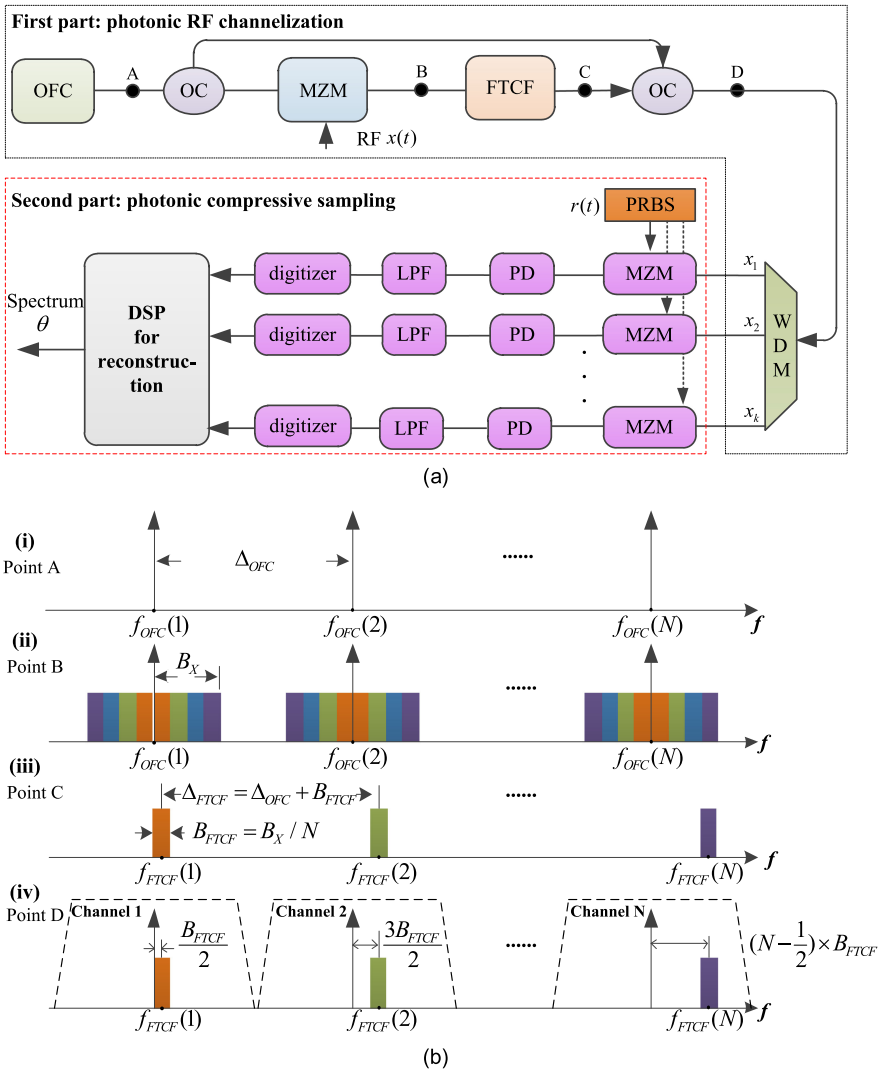

Fig. 1. (a) Configuration of the broadband microwave spectrum sensing based on photonic RF channelization and compressive sampling. OFC: optical frequency comb, OC: optical coupler, MZM: Mach–Zehnder modulator, FTCF: flat-top optical comb filter, WDM: wavelength-division multiplexer, PRBS: pseudo-random binary sequence, PD: photodetector, LPF: low pass filter, DSP: digital signal processer. (b) Principle of the proposed photonic RF channelization, (i): the spectrum of the OFC at point A, (ii): the spectrum of the OFC modulated by the input signal at point B, (iii): the spectral components sliced by the FTCF at point C, (iv): the spectrum of the combined signal before the WDM at point D.

the lower path, the OFC is modulated by a broadband RF signal to be measured via an MZM, and then spectrally sliced by a FTCF. In the upper path, the OFC is unchanged. The signals in the two paths are recombined by a second OC. Finally, A wavelength-division multiplexer (WDM) is used to separate the different channels physically. The principle of RF spectrum slicing and channelization is shown in Fig. 1(b).

The frequency of each line in OFC can be express as $f_{OFC}(k) = f_{OFC}(1) + (k-1)\Delta_{OFC}$, where $f_{OFC}(1)$ and $f_{OFC}(k)$ mean the frequencies of the first line and the k-th line, Δ_{OFC} is the line spacing. Assume that the MZM is driven by an RF signal with maximum frequency of B_X under the small signal driving and double-sideband modulation. The RF signal is then multi-cast by the comb and the k-th up-converted copy has the frequencies of $f_{OFC}(1) + (k-1)\Delta_{OFC} \pm B_X$. For the FTCF, its

free spectral range (FSR) and 3 dB bandwidth are Δ_{FTCF} and B_{FTCF}, respectively, the FSR Δ_{FTCF} is set to be $\Delta_{OFC} + B_{FTCF}$, the B_{FTCF} is set to be B_X/N, N is the channelization factor of the photonic RF channelizer. The k-th transmission peak of the FTCF can be expressed as $f_{FTCF}(k) = f_{FTCF}(1) + (k-1)\Delta_{FTCF}$. The combined signal is separated by a WDM with a channel spacing of Δ_{OFC} and the signal in each sub-channel is sent to mix with the PRBS prior to a PD. When the frequency of the first line in the OFC $f_{OFC}(1)$ is tuned to be $f_{FTCF}(1) - B_{FTCF}/2$, as shown in Fig. 1(b), the center frequency of the microwave signal x_k in k-th sub-channel detected by PD can be expressed as

$$\begin{aligned} f_c(k) &= f_{FTCF}(k) - f_{OFC}(k) \\ &= f_{FTCF}(1) - f_{OFC}(1) + (k-1)(\Delta_{FTCF} - \Delta_{OFC}) \\ &= f_{FTCF}(1) - f_{OFC}(1) + (k-1)B_{FTCF} \\ &= (k - 1/2) \times B_{FTCF} \end{aligned} \tag{1}$$

As a result, the output microwave signal of the first sub-channel has a center frequency of $B_{FTCF}/2$ and a bandwidth of B_{FTCF}, and the output signal of the last sub-channel has a center frequency of $N \times B_{FTCF} - B_{FTCF}/2$ and a bandwidth of B_{FTCF}. In the process of photonic RF channelization, the input broadband signal is sliced into N sub-channels while each sub-channel has a bandwidth of B_{FTCF}. It should be mentioned that the center frequency of each sub-channel can be changed by tuning the frequency of the OFC or the transmission peak of the FTCF.

The second part is the photonic CS modules based on bandpass sampling and random demodulator. The channelized signal is mixed with a PRBS which is a random series of digital 1's and 0's within the sequence length. Then the detected electrical signal passes through a low-pass filter (LPF) and is then down-sampled by a digitizer with a sampling rate much lower than the rate of the PRBS. At last, a digital signal processer (DSP) is used for signal construction with the help of a sparse recovery algorithm.

Since the outputs from the sub-channels are bandpass signals, we employ bandpass sampling to decrease the bandwidth of the CS system. After channelization, the bandwidth of the input signal is decreased by N fold to be B_{FTCF}. According to the theory of bandpass sampling [29], the Nyquist rate should be $2 \times B_{FTCF}$ or higher to avoid frequency aliasing for a bandpass signal with a bandwidth of B_{FTCF}. On the other hand, the clock rate of the PRBS in random demodulator must be at or higher than the Nyquist rate, that is, the clock rate of the PRBS should be $2 \times B_{FTCF}$ or higher.

In our approach, the channelization factor of the photonic RF channelizer is N, the clock rate f_s of the PRBS $r(t)$ at the stage of random mixing can be slowed down to be $1/N$ of the Nyquist rate f_{NQ} of $x(t)$.

$$f_s = \frac{f_{NQ}}{N} \tag{2}$$

If the compression factor of the CS system is R_{CS}, the random modulated signal $x_k \times r(t)$ passes through the LPF and is digitized by every R_{CS} samples, which means the actual sampling rate of the digitizer f_d can be expressed as

$$f_d = \frac{f_{NQ}}{N \times R_{CS}} \tag{3}$$

For the first sub-channel, the process of CS measurement can be modeled by $y = DHRx_1 = DHRW_1\theta$, where $x_1 = W_1\theta$ is a column vector with length I (each entry corresponds to a sample at the rate of f_s), W_1 is a $I \times I$ matrix denoting the Fourier orthogonal basis, $W_1 \in [0, B_{FTCF}]$, θ is a $I \times 1$ vector denoting the spectrum information of x_1, R is a $I \times I$ matrix denoting the mixing by the PRBS $r(t)$, H is a $I \times I$ matrix denoting the impulse response of the LPF, and D is a $J \times I$ matrix denoting the down-sampling of the digitizer ($I = J \times R_{CS}$). D, H and R can be determined by the parameters of the down-sampling, LPF and PRBS, and y is the measurement result, θ can be solved as a minimization problem by a sparse recovery algorithm given that θ is sparse in W_1.

For the k-th sub-channel, the only difference with the first sub-channel is that the x_k with frequency at $[(k-1)B_{FTCF}, k \times B_{FTCF}]$ is firstly spectrally down-shifted to $[0, B_{FTCF}]$ by the PRBS with bandpass

sampling. According to the theory of bandpass sampling, the horizontal axes of the recovered spectrum θ for k-th sub-channel should be rescaled as Eq. (4), where $\lfloor k/2 \rfloor$ is round down $k/2$, $W_k \in [(k-1)B_{FTCF}, k \times B_{FTCF}]$

$$W_k = 2 \times \lfloor k/2 \rfloor \times B_{FTCF} + (-1)^{(k-1)} W_1 \tag{4}$$

Finally, the spectrum of the input broadband signal to be measured can be obtained by splicing the spectra in all the sub-channels into a complete one.

3. Results and Discussions

Simulations are carried out to demonstrate the proposed approach for spectrum sensing of the signal with a bandwidth of 40 GHz. The Nyquist rate f_{NQ} corresponding to this bandwidth is 80 GHz, which is far beyond the sampling rate of the digitizers available today. The parameters related to the photonic RF channelizer in the simulation are set as follows, $\Delta_{OFC} = 90$ GHz, $\Delta_{FTCF} = 100$ GHz, $B_X = 40$ GHz, $B_{FTCF} = 10$ GHz, $N = 4$. The input broadband microwave signal is sliced into four sub-channels, each with a bandwidth of 10 GHz, by the photonic RF channelizer. The parameters for the CS modules are as follows: $I = 1024$, $R_{CS} = 8$ and $J = I/R_{CS} = 128$. The impulse response of the LPF H is a 1024×1024 matrix set as in [21]. The length of the finite impulse response is typically chosen to be 8, and the LPF is equivalent to an integrator that sums 8 discrete values of $x_k \times r(t)$. In the simulation, we use the sparse recovery algorithm developed by Figueiredo *et al.* [33]. The above parameters mean that the rate of the PRBS in the CS modules is $f_s = f_{NQ}/N = 20$ Gbit/s and the actual sampling rate of the digitizer is $f_d = f_{NQ}/N/R_{CS} = 2.5$ GS/s.

First, we test the case of an input signal with four tones, i.e. 3 GHz, 14 GHz, 25 GHz, and 36 GHz, corresponding to one tone in each sub-channel after the WDM. The original spectrum with Nyquist sampling is shown in Fig. 2(a). The recovered spectrum θ in each sub-channel by the bandpass sampling CS is shown in Fig. 2(b). The bandwidth of all sub-channels are 10 GHz and the recovered frequency in each sub-channel is respectively 3 GHz, 6 GHz, 5 GHz, and 4 GHz. According to Eq. (4), the horizontal axes of the recovered spectrum θ for sub-channels 2, 3, 4 are rescaled as shown in Fig. 2(c). It is seen that the recovered frequencies are accurate and the recovery performance is pretty good. Note that the fluctuation of the amplitude for different spectral components is attributed to the frequency basis mismatch in discrete Fourier transform [34].

Next, the case of an input signal with multi-tones in each sub-channel is considered. We assume that the input signal includes ten spectral components, i. e. 3, 5, 10.95, 15, 19, 21, 25, 29.1, 35, and 39 GHz. It should be pointed out that the frequencies of 10.95, 19, 21, 29.1 GHz are at the edge of the sub-channels, which will fall into adjacent two sub-channels since the transmission function of the FTCF in one FSR is not ideal rectangle shape. Therefore, the edge roll-off property of the applied FTCF may have major impact on the performance of spectrum sensing. The edge roll-off property of the applied FTCF can be quantitatively described as the shape factor (SF), which is defined as the ratio of the 40-dB bandwidth to the 6-dB bandwidth. Two FTCFs with different SF, i.e, 2.5 and 1.7, are chosen in the simulation to evaluate the influence of the out-of-band leakage induced by non-ideal filters. The FTCF with these SFs can be obtained with apodized coupled resonator waveguides and are commercially available [35]–[38]. The power transmission responses of the two FTCFs are shown in Fig. 3. It is seen a lower SF corresponds to a sharper edge.

Fig. 4 shows the simulation results for the case of multi-tones in each sub-channel. The spectrum of the input signal is shown in Fig. 4(a). The recovered spectrum corresponding to the system using an FTCF with SF $= 2.5$ is shown Fig. 4(b); fig. 4(c) corresponds to the case of an FTCF with SF $= 1.7$. It is found in Fig. 4(b) that the spectrum recovery is also very good except for two alias frequencies appear. Essentially, the spectral leakage in the sub-channel edges will cause frequency aliasing in the bandpass sampling with the relatively low rate PRBS. The alias frequency at 9.05 GHz is actually 10.95 GHz which is down-shifted to 9.05 GHz by band-pass sampling. Since the filter edge is not steep enough, the frequency 10.95 GHz supposed to be in second sub-channel leaks to the first sub-channel. The alias frequency at 30.9 GHz is actually 29.1 GHz for the same reason. When the FTCF with a sharper edge (SF $= 1.7$) is applied, the alias frequencies near the

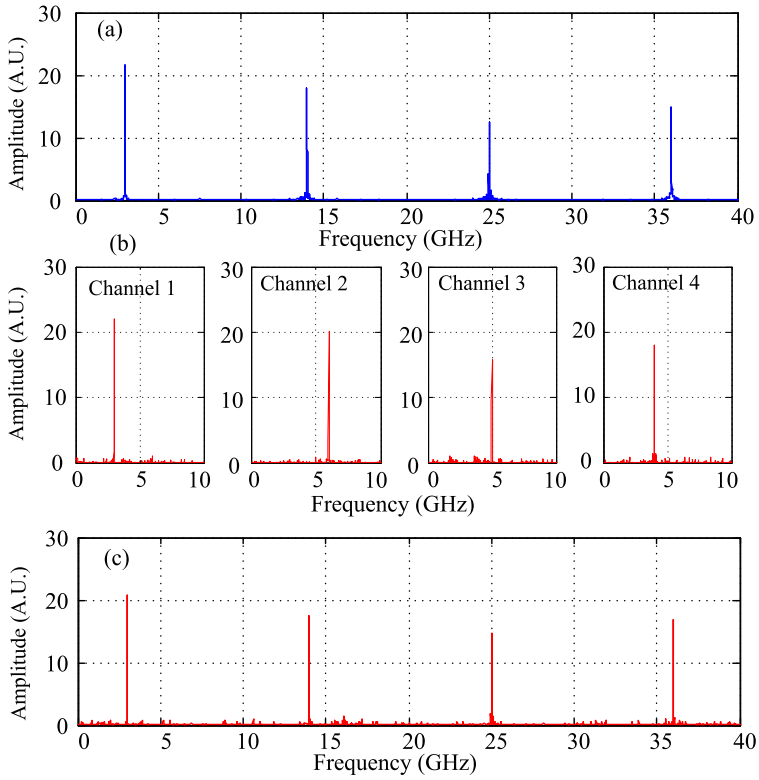

Fig. 2. Simulation results of single tone input in each sub-channel. (a) Spectrum of the original signal. (b) Spectrum of the recovered signal of each sub-channel before horizontal axes rescaled. (c) Spectrum of the recovered signal.

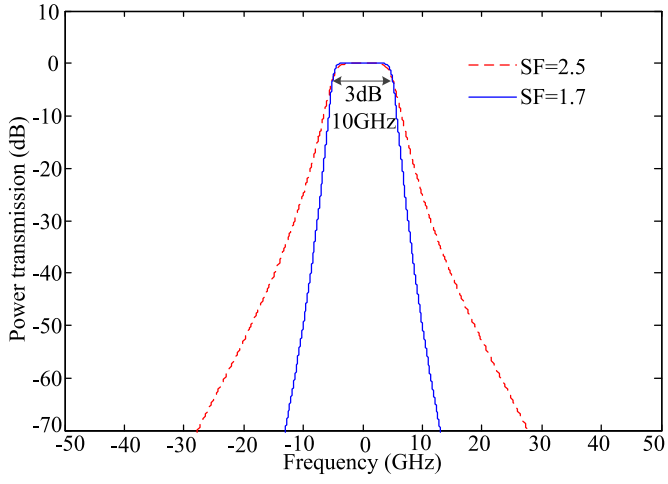

Fig. 3. The power transmission of the flat-top optical comb filter (FTCF) in one FSR.

sub-channel edges are suppressed to the noise level, as shown in Fig. 4(c). It proves that the alias frequencies are due to the spectral leakage between adjacent sub-channels and the use of FTCF with a shaper roll-off can reduce the leakage.

It is demonstrated that a high-performance FTCF can be used to alleviate the problem of the out-of-band spectral leakage. Here we present another approach to completely avoid the problem of spectral leakage in the sub-channel edges. In this approach, the ranges of the alias frequency

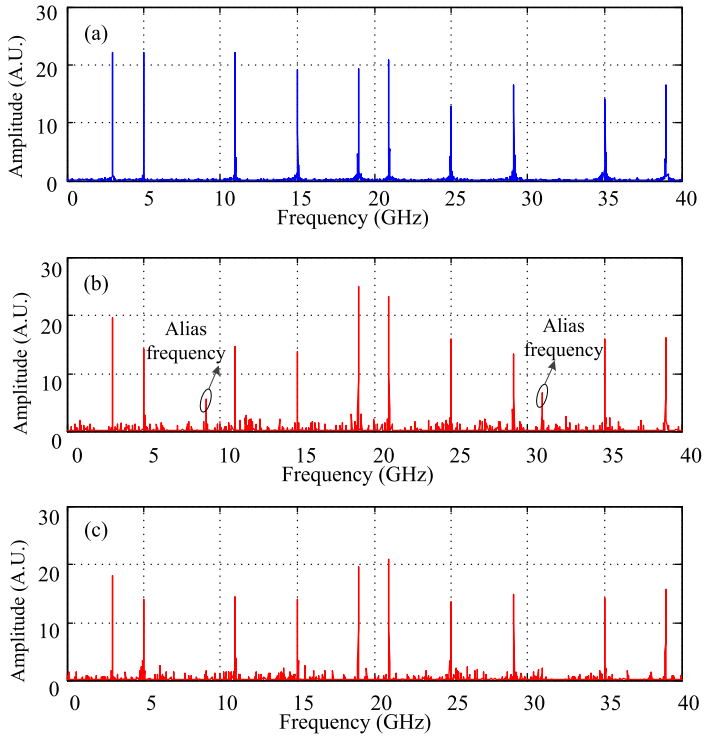

Fig. 4. Simulation results of multiple tones input in each sub-channel. (a) Spectrum of the original signal. (b) Spectrum of the recovered signal with an SF = 2.5 FTCF. (c) Spectrum of the recovered signal with an SF = 1.7 FTCF.

caused by spectral leakage are set different by measuring twice and the original signal can be recovered through extracting the common spectral components in the two measurements. For the simplicity of analysis, the bandwidth of frequency overlaps between adjacent sub-channels is calculated to be 2 GHz when the FTCF with SF = 2.5 is used. In the first measurement, the center frequency of each sub-channel is left-shifted by 1/2 bandwidth of the frequency overlap (1 GHz) by tuning the frequency of the OFC with $f_{FTCF}(1) = f_{OFC}(1) + B_{FTCF}/2 - 1$; the ranges of the alias frequency are set to be 10∼12, 20∼22, and 30∼32 GHz. In the second measurement, the center frequency of each sub-channel is right-shifted by 1/2 bandwidth of the frequency overlap (1 GHz) by tuning the frequency of the OFC with $f_{FTCF}(1) = f_{OFC}(1) + B_{FTCF}/2 + 1$; the ranges of the alias frequency are 8∼10, 18∼20, and 28∼30 GHz. Since the ranges of the alias frequency are different in two measurements, the broadband microwave spectrum can be recovered without frequency ambiguity through extracting the common spectral components in two measurements. The results are presented in Fig. 5. The common spectral components in two measurements are 3, 5, 10.95, 15, 19, 21, 25, 29.1, 35, and 39 GHz, which is consistent with the original spectrum.

It should be mentioned that the optimum channelization factor *N* needs further discussion for different applications. In one hand, with the increase of the channelization factor *N*, the rate of PRBS and the bandwidth of the MZM for CS can be largely decreased while the numbers of the PD, LPF, and digitizer are increased simultaneously. Besides, with the increase of the channelization factor *N,* the crosstalk between different channels will increase and cause degradation of the signal to noise ratio which may limit the signal recovery performance of CS [27].

4. Summary

We have proposed a novel approach for broadband microwave spectrum sensing which combines the photonic RF channelization and compressive sampling. These two techniques help to largely

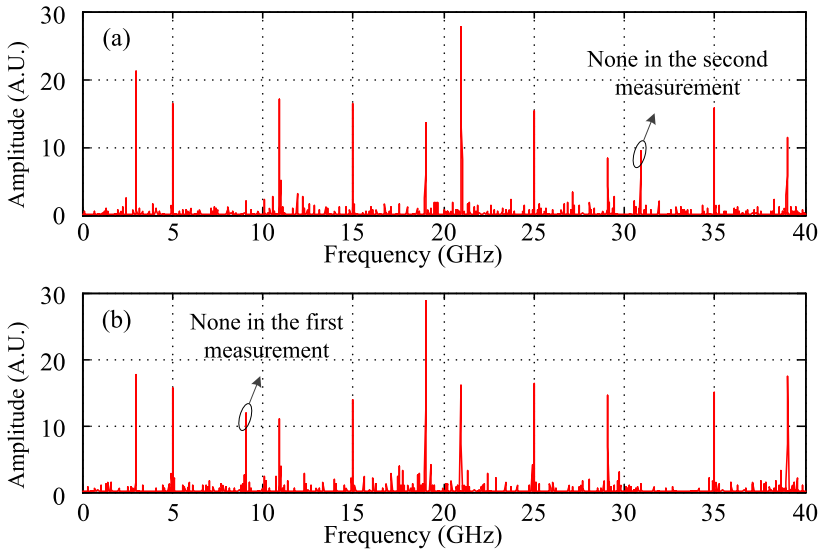

Fig. 5. Simulation results of multiple tones input in each sub-channel with 2.5 SF FTCF. (a) Spectrum of the recovered signal with center frequency of each sub-channel left shifted by 1 GHz. (b) Spectrum of the recovered signal with center frequency of each sub-channel right shifted by 1 GHz.

decrease the sampling rate of the digitizer required for the spectrum sensing and signal reconstruction. The photonic RF channelizer slices the input broadband signal into multiple sub-channels with narrow bandwidth and then effectively decreases the clock rate of the PRBS and the bandwidth of the mixer in the random demodulator. The influence of the non-rectangular-shape filter response in the channelization is evaluated. We also proposed an approach based on measuring twice to overcome the frequency aliasing problem induced by the non-ideal response of filter. All the components used in the given scheme are commercially available. We believe it has potential applications in the microwave spectrum sensing with ultra-wide bandwidth.

Acknowledgment

The authors would like to thank the anonymous reviewers for their valuable suggestions.

References

[1] L. V. T. Nguyen and D. B. Hunter, "A photonic technique for microwave frequency measurement," *IEEE Photon. Technol. Lett.*, vol. 18, no. 10, pp. 1188–1190, May 2006.
[2] H. Chi, X. Zou, and J. Yao, "An approach to the measurement of microwave frequency based on optical power monitoring," *IEEE Photon. Technol. Lett.*, vol. 20, no. 14, pp. 1249–1251, Jul. 2008.
[3] S. Pan, J. Fu, and J. Yao, "Photonic approach to the simultaneous measurement of the frequency, amplitude, pulse width, and time of arrival of a microwave signal," *Opt. Lett.*, vol. 37, no. 1, pp. 7–9, 2012.
[4] B. Vidal, T. Mengual, and J. Marti, "Photonic technique for the measurement of frequency and power of multiple microwave signals," *IEEE Trans. Microw. Theory Techn.*, vol. 58, no. 11, pp. 3103–3108, Nov. 2010.
[5] S. Winnall and A. Lindsay, "A Fabry–Perot scanning receiver for microwave signal processing," *IEEE Trans. Microw. Theory Techn.*, vol. 47, no. 7, pp. 1385–1390, Jul. 1999.
[6] M. Pelusi *et al.*, "Photonic-chip-based radio-frequency spectrum analyser with terahertz bandwidth," *Nature Photon.*, vol. 3, no. 3, pp. 139–143, 2009.
[7] P. Rugeland, Z. Yu, C. Sterner, G. Tarasenko, and W. Margulis, "Photonic scanning receiver using an electrically tuned fiber Bragg grating," *Opt. Lett.*, vol. 34, no. 24, pp. 3794–3796, 2009.
[8] D. B. Hunter, L. G. Edvell, and M. A. Englund, "Wideband microwave photonic channelised receiver," in *Proc. Int. Top. Meeting Microw. Photon.*, 2005, pp. 249–252.
[9] X. Zou, W. Pan, B. Luo, and L. S. Yan, "Photonic approach for multiple-frequency-component measurement using spectrally sliced incoherent source," *Opt. Lett.*, vol. 35, no, 3, pp. 438–440, 2010.
[10] K. K. Xu *et al.*, "Light emission from a poly-silicon device with carrier injection engineering," *Mater. Sci. Eng., B*, vol. 231, pp. 28–31, 2018.

[11] T. Steinmetz *et al.*, "Laser frequency combs for astronomical observations," *Science*, vol. 321, no. 5894, pp. 1335–1337, 2008.
[12] Z. Li, H. Chi, X. Zhang, S. Zheng, X. Jin, and J. Yao, "A reconfigurable photonic microwave channelized receiver based on an optical comb," in *Proc. Int. Top. Meeting Microw. Photon., Jointly Held Asia-Pacific Microw. Photon. Conf.*, Singapore, 2011, pp. 296–299.
[13] X. Xie *et al.*, "Broadband photonic radio-frequency channelization based on a 39-GHz optical frequency comb," *IEEE Photon. Technol. Lett.*, vol. 24, no. 8, pp. 661–663, Apr. 2012.
[14] H. Chen *et al.*, "Photonics-assisted serial channelized radio-frequency measurement system with Nyquist-bandwidth detection," *IEEE Photon. J.*, vol. 6, no. 6, Dec. 2014, Art. no. 7903707.
[15] X. Xie *et al.*, "Broadband photonic RF channelization based on coherent optical frequency combs and I/Q demodulators," *IEEE Photon. J.*, vol. 4, no. 4, pp. 1196–1202, Aug. 2012.
[16] Y. Han and B. Jalali, "Photonic time-stretched analog-to-digital converter: Fundamental concepts and practical considerations," *J. Lightw. Technol.*, vol. 21, no. 12, pp. 3085–3103, Dec. 2003.
[17] P. W. Juodawlkis, J. J. Hargreaves, R. D. Younger, G. W. Titi, and J. C. Twichell, "Optical down-sampling of wide-band microwave signals," *J. Lightw. Technol.*, vol. 21, no. 12, pp. 3116–3124, Dec. 2003.
[18] J. Kim, M. J. Park, M. H. Perrott, and F. X. Kartner, "Photonic subsampling analog-to-digital conversion of microwave signals at 40-GHz with higher than 7-ENOB resolution," *Opt. Express*, vol. 16, no. 21, pp. 16509–16515, 2008.
[19] G. C. Valley, "Photonic analog-to-digital converters," *Opt. Express*, vol. 15, no. 5, pp. 1955–1982, 2007.
[20] Z. P. Zhang *et al.*, "Silicon light-emitting device for high speed analog-to-digital conversion," *J. Optoelectronics Adv. Mater.*, vol. 18, no. 9-10, pp. 737–744, 2016.
[21] J. M. Nichols and F. Bucholtz, "Beating Nyquist with light: A compressively sampled photonic link," *Opt. Express*, vol. 19. no. 8, pp. 7339–7348, 2011.
[22] H. Nan, Y. Gu, and H. Zhang, "Optical analog-to-digital conversion system based on compressive sampling," *IEEE Photon. Technol. Lett.*, vol. 23, no. 2, pp. 67–69, Jan. 2010.
[23] C. Wang and N. J. Gomes, "Photonics-enabled sub-Nyquist radio frequency sensing based on temporal channelization and compressive sensing," in *Proc. Microw. Photon., 9th Asia-Pacific Microw. Photon. Conf.*, 2014, pp. 335–338.
[24] F. F. Yin *et al.*, "Multifrequency radio frequency sensing with photonics-assisted spectrum compression," *Opt. Lett.*, vol. 38, no. 21, pp. 4386–4388, 2013.
[25] Y. H. Liang, M. H. Chen, H. W. Chen, C. Lei, P. X. Li, and S. Z. Xie, "Photonic-assisted multi-channel compressive sampling based on effective time delay pattern," *Opt. Express*, vol. 21, no. 22, pp. 25700–25707, 2013.
[26] G. C. Valley, G. A. Sefler, and T. J. Shaw, "Compressive sensing of sparse radio frequency signals using optical mixing," *Opt. Lett.*, vol. 37, no. 22, pp. 4675–4677, 2012.
[27] H. Chi, Y. Chen, Y. Mei, X. F. Jin, S. L. Zheng, and X M. Zhang, "Microwave spectrum sensing based on photonic time stretch and compressive sampling," *Opt. Lett.*, vol. 38, no. 2, pp. 136–138, 2013.
[28] B. T. Bosworth and M. A. Foster, "High-speed ultrawideband photonically enabled compressed sensing of sparse radio frequency signals," *Opt. Lett.*, vol. 38, no. 22, pp. 4892–4895, 2013.
[29] Z. J. Zhu, H. Chi, S. L. Zheng, T. Jin, X. F. Jin, and X. M. Zhang, "Analysis of compressive sensing with optical mixing using a spatial light modulator," *Appl. Opt.*, vol. 54, no. 8, pp. 1894–1899, 2015.
[30] M. Mishali and Y. C. Eldar, "From theory to practice: Sub-Nyquist sampling of sparse wideband analog signals," *IEEE J. Sel. Topics Signal Process.*, vol. 4, no. 2, pp. 375–391, Apr. 2010.
[31] S. Kirolos *et al.*, "Analog-to-information conversion via random demodulation," in *Proc. IEEE Dallas/CAS Workshop Des., Appl., Integr. Softw.*, 2006, pp. 71–74.
[32] D. M. Akos, M. Stockmaster, J. B. Y. Tsui, and J. Caschera, "Direct bandpass sampling of multiple distinct RF signals," *IEEE Trans. Commun.*, vol. 47, no. 7, pp. 983–988, Jul. 1999.
[33] M. A. T. Figueiredo, R. D. Nowak, and S. J. Wright, "Gradient projection for sparse reconstruction: Application to compressed sensing and other inverse problems," *IEEE J. Sel. Topics Signal Process.*, vol. 1, no. 4, pp. 586–597, Dec. 2007.
[34] C. V. McLaughlin, J. M. Nichols, and F. Bucholtz, "Basis mismatch in a compressively sampled photonic link," *IEEE Photon. Technol. Lett.*, vol. 25, no. 23, pp. 2297–2300, Dec. 2013.
[35] K. K. Xu, "Silicon MOS optoelectronic micro-nano structure based on reverse-biased PN junction," *Physica Status Solidi (A)*, vol. 216, no. 7, 2019, Art. no. 1800868.
[36] J. Capmany, P. Muñoz, J. D. Domenech, and M. A. Muriel, "Apodized coupled resonator waveguides," *Opt. Express*, vol. 15, no. 16, pp. 10196–10206, 2007.
[37] K. K. Xu, Y. X. Chen, T. A. Okhai, and L. W. Snyman, "Micro optical sensors based on avalanching silicon light-emitting devices monolithically integrated on chips," *Opt. Mater. Express*, vol. 9, no. 10, pp. 3985–3997, 2019.
[38] Y. Chen and B. Steve, "Nonlinearity enhancement in finite coupled-resonator slow-light waveguides," *Opt. Express*, vol. 12, no. 15, pp. 3353–3366, 2004.